2008 American Control Conference
Westin Seattle Hotel, Seattle, Washington, USA
June 11-13, 2008

Swarming Control Using Parallel Gibbs Sampling

Xiaobo Tan

Abstract— **In the prior work of the author and his coworkers, Gibbs sampling was proposed for coordination of autonomous swarms, where convergence results were only obtained for sequential sampling with additional requirement of modest global communication. In this paper the convergence behavior is investigated under parallel Gibbs sampling, where all mobile nodes update their locations simultaneously. It is established that, with a pairwise Gibbs potential, parallel Gibbs sampling and annealing minimizes a modified potential energy, where the extent of modification is determined by the maximum travel range of each node within one time step. This is the first convergence result for parallel sampling algorithms for Gibbs random fields with configuration-dependent neighborhood systems, and it provides justification for Gibbs sampling as a viable method for swarming control. The latter is further illustrated with simulation results.**

I. Introduction

Rapid technological advances have made it possible to build and deploy a large number of mobile robots or unmanned vehicles at an affordable cost. Networks of such autonomous vehicles can have a multitude of military and civil applications, ranging from surveillance and reconnaissance, to search and rescue, to weather forecast, and to oceanography. It is intriguing to endow big groups of autonomous vehicles (called *autonomous swarms* in this paper) with emergent properties, i.e., to achieve global goals (e.g., pattern formation, rendezvous, or maximum coverage area) through distributed, limited, local communication and computation. This is dictated by the otherwise prohibitive cost for centralized coordination of large-scale networks, and by the need to ensure robustness against single-node failures.

Recent years have witnessed significant advances in the area of multi-agent coordination and control, where tools from control and dynamical systems theory and algebraic graph theory are applied to formally analyze or synthesize interaction rules for mobile agents. It is notable that a number of convergence results accommodating time-varying communication topology have been obtained [1]–[5]. Despite the progress made, most results provide only convergence to local minima of potential or objective functions [5]–[8], and global objectives are achievable only if initial configurations are sufficiently close to the desired ones. There are a few results on global convergence [1], [2], [4]; however, they all require global connectedness of the network (to some varying degrees), which is not guaranteed by the algorithms.

Baras and Tan [9] proposed a Markov random fields (MRFs)-based framework for the coordination of autonomous swarms with the goal of achieving global objectives using purely local interactions. In that approach vehicles are allowed to move on a discretized lattice, and the moving decisions are made through Gibbs sampling based on local information perceived by individual vehicles. The neighborhood systems associated with swarm MRFs vary with configurations. This represents a key difference from classical MRF theory [10], [11], which deals with only fixed neighborhood systems. In the prior work of the author and his coworkers [12], rigorous convergence proof was only obtained for sequential Gibbs sampling (updating one node at a time) with an additional assumption that global communication is available for forwarding relevant information to newly selected node at each time step. Sequential sampling, however, is not feasible in practice: 1) it takes too long to complete one round of updating for large vehicle networks, and 2) it requires explicit indexing of nodes, which is often impossible due to dynamic addition/removal of nodes. The global communication requirement, despite the limited information transmitted, defeats the goal of full decentralization.

This paper concerns the convergence behavior of swarming control algorithms based on parallel Gibbs sampling, where nodes update their locations simultaneously. For the important case of pairwise Gibbs potentials, an explicit expression is derived for the (unique) stationary distribution of swarm configurations under fixed-temperature sampling, which takes a *quasi-Gibbsian* form. We further characterize the convergence behavior of the swarm configuration under an appropriate annealing schedule. In particular, it is shown that parallel annealing minimizes an energy function modified from the original Gibbs potential energy, and the extent of modification is determined by the maximum travel distance R_m per time step for each node. Interpreted physically, the result implies that more frequent information exchange (smaller R_m) leads to configurations closer to states which minimize the original energy function.

The result is the first of its kind for parallel Gibbs sampling algorithms for MRFs with configuration-dependent neighborhood systems. It provides an explanation for the promising simulation results observed first in [9], and offers justification and guidance on using Gibbs sampling as a viable, decentralized method for swarming control.

The remainder of the paper is organized as follows. In Section II, the background on MRFs is reviewed and the application of MRFs to modeling of autonomous swarms is described. Analysis of the parallel sampling algorithm is carried out in Section III. Simulation results are presented in Section IV. Finally Section V provides concluding remarks.

X. Tan is with the Department of Electrical and Computer Engineering, Michigan State University, East Lansing, MI 48824, USA. xbtan@egr.msu.edu

978-1-4244-2079-7/08/$25.00 ©2008 AACC.

II. MRFs and Application to Swarming Control

A. Review of Classical MRFs and Gibbs Sampling

MRFs form a natural generalization of Markov processes with the temporal index replaced by a spatial index, and provide a framework for investigating local interactions. Initially proposed by Ernst Ising with an attempt to explain ferromagnetism [13], MRFs have since been applied to the study of statistical physics, biology, economics, and sociology [10], and in particular, to image processing and computer vision with great success [11], [14].

1) MRFs: Let S be a set of *sites* indexed by s. A *random field* is a collection $X = \{X_s\}_{s\in S}$ of random variables, with X_s taking values in Λ_s, the *phase space* for site s. A realization $x = \{x_s\}_{s\in S}$ of X is called a *configuration* or *state*. A *neighborhood system* on S is a family $\Gamma = \{\Gamma_s\}_{s\in S}$, where $\Gamma_s \subset S$ is the set of neighbors for site s satisfying $s \notin \Gamma_s$ and $r \in \Gamma_s \Leftrightarrow s \in \Gamma_r$. The neighborhood system induces an undirected graph with vertices $s \in S$, and an edge exists between s and r if and only if $r \in \Gamma_s$. A set $C \subset S$ is called a *clique* if all elements of C are neighbors of each other. The random field X is called a *Markov random field* (MRF) with respect to the neighborhood system Γ if, $\forall s \in S$,

$$P(X_s = x_s | X_r = x_r, r \neq s) = P(X_s = x_s | X_r = x_r, r \in \Gamma_s). \quad (1)$$

The righthand side of (1) is often referred to as the *local characteristics* of the MRF.

A *potential* U is a family $\{U_A : A \subset S\}$ of functions on the configuration space, where $U_A(x)$ depends only on $x_A \stackrel{\triangle}{=} \{x_s : s \in A\}$; with a bit of notation abuse, we will write $U_A(x_A) \stackrel{\triangle}{=} U_A(x)$. If $U_A = 0$ whenever A is not a clique or a singleton, U is called a *nearest-neighbor* potential. If $U_A = 0$ whenever A is not a pair or a singleton, U is called a *pairwise* potential. Given a potential U, the *energy* $H(x)$ is defined as

$$H(x) = \sum_{A\subset S} U_A(x). \quad (2)$$

A random field X is called a *Gibbs random field* if

$$P(X = x) = \frac{e^{-H(x)/T}}{Z}, \quad \text{with } Z = \sum_z e^{-H(z)/T}. \quad (3)$$

T has the interpretation of temperature in the context of statistical physics. The Hammersley-Clifford theorem establishes the equivalence between an MRF and a Gibbs field, which provides a tangible, convenient characterization of MRFs through potentials.

2) Gibbs Sampling: While a Gibbs field describes the system behavior at the thermodynamic equilibrium, direct evaluation of (3) and related ensemble averages is often impossible due to the high cardinality of the configuration space (the latter rendering the computation of Z intractable). Markov Chain Monte Carlo (MCMC) methods, such as the Metropolis algorithm [15] and the Gibbs sampler [16], can generate Markov chains on the configuration space, with (3) as the limiting probability measure. Take the *Gibbs sampler*. Pick a site s. Given the current configuration x, one updates it to a new configuration y by replacing x_s with y_s, where y_s is obtained by sampling the local characteristics of (3) at site s:

$$P(X_s = y_s | X_{S\backslash s} = x_{S\backslash s}) = \frac{e^{-H(y_s, x_{S\backslash s})/T}}{\sum_{z_s} e^{-H(z_s, x_{S\backslash s})/T}}, \quad (4)$$

where $S\backslash s \stackrel{\triangle}{=} \{r \in S : r \neq s\}$ is the set of all sites except s. Note that the evaluation of (4) involves only $\{x_r : r \in \Gamma_s\}$ for a Gibbs field with nearest-neighbor potential. One can update all sites sequentially in a prescribed order, which generates a (homogeneous) Markov chain with transition probabilities $\mathscr{P}(x,y)$. $\mathscr{P}$ satisfies the *detailed balance* equation:

$$P(x)\mathscr{P}(x,y) = P(y)\mathscr{P}(y,x), \quad (5)$$

implying that the Gibbs measure $P(x)$ is the (unique) stationary distribution for the Gibbs sampling-induced Markov chain.

3) Stochastic Relaxation: The Gibbs distribution (3) depends on the temperature T. The lower T is, the higher probabilities for lowest-energy configurations. In the limit of $T \to 0$, (3) produces probabilities concentrating solely on configurations of minimum energy. Taking the idea of simulated annealing [17], Geman and Geman proposed decreasing T gradually during Gibbs sampling and established the convergence to the lowest-energy configurations [16].

B. Modeling Autonomous Swarms by MRFs

Inspired by the MRFs' capability in modeling local interactions, Baras and Tan introduced the concepts of MRFs and Gibbs sampling into the context of autonomous swarms [9]. Consider a group of mobile vehicles moving in 2D or 3D space, which is discretized into a lattice. For ease of presentation, each cell is assumed to be square with unit dimensions. A vehicle is assumed to be a point that moves from the center of one cell to that of another. Each vehicle has a *sensing range* R_s: it can sense the locations of obstacles and other vehicles within distance R_s. It also has an *interaction range* $R_i \leq R_s$: the moving decision of a vehicle is only influenced by vehicles within the distance R_i, which form its set of *neighbors*. In addition, each vehicle can travel by at most $R_m \leq R_s$ within each time step. The distances on the lattice are defined using the Euclidean norm based on the center locations of cells.

The R_i-neighborhood relations induce a graph structure, where the vehicles form the vertices of the graph and an edge exists between two vehicles if and only if they are neighbors of each other. An MRF is then defined on this graph, where each vehicle s is a site. Define the set of sites $S \stackrel{\triangle}{=} \{1, \cdots, N_v\}$, where N_v is the total number of vehicles. The set of lattice cells within R_m from vehicle s form the phase space Λ_s. In particular, x_s (or y_s, z_s, etc.) will denote the center location of the cell in which node s resides. A potential U is defined to reflect the coordination/control objectives, from which the energy H can be evaluated.

The MRF defined for an autonomous swarm, *a swarm MRF* for short, is fundamentally different from a traditional MRF in that the latter has a fixed, prescribed neighborhood

system. The neighborhood system for a swarm MRF, on the other hand, is determined by the distances between vehicles and varies with the swarm configuration. We will denote by $\Gamma_s(x)$ the set of neighbors of node s given the configuration x. The interaction graph is thus a proximity graph [18] or a state-dependent dynamic graph [19], which is typical for multi-agent networks. Consequently, a number of challenges arise in the study of swarm MRFs since the classical MRF theory does not apply directly. First, even with sequential sampling, the detailed balance (5) no longer holds and the Gibbs distribution is no longer the stationary distribution. Second, due to feasibility considerations, one is interested in a swarm MRF's convergence behavior under parallel sampling, which is very involved even for classical MRFs [11]. Xi *et al.* [12] conducted analysis for a special sequential sampling scheme with an assumption on limited global communication. In this paper we consider the case of parallel sampling with purely local interactions.

III. Analysis of Parallel Gibbs Sampling Scheme

A. Parallel Sampling Algorithm

Let n denote the index of time steps. Let $X(n) = x = (x_1, \cdots, x_S)$ be the current swarm configuration. Let $F_s(x) \triangleq \{z_s : \|z_s - x_s\| \le R_m\}$ be the set of accessible cell locations for node s given the configuration x, determined by the mobility constraint. Let $F(x) \triangleq \{z : \|z_s - x_s\| \le R_m, \forall s\}$ be the set of configurations that are accessible from x within one time step. Under parallel Gibbs sampling, all nodes will simultaneously update their locations based on the configuration x at time n; in particular, the node s will move from x_s to y_s at time $n+1$ with probability

$$P_s^T(x_s, y_s) = \begin{cases} \frac{e^{-\frac{H(y_s, x_{S\setminus s})}{T}}}{\sum_{z_s \in F_s(x)} e^{-\frac{H(z_s, x_{S\setminus s})}{T}}} & \text{if } y_s \in F_s(x) \\ 0 & \text{if } y_s \notin F_s(x) \end{cases}. \quad (6)$$

For simulated annealing, the temperature variable T will be a function of the time step n. The following assumptions are made:

- $(\mathbf{A_1})$ The total number N of lattice cells is bounded;
- $(\mathbf{A_2})$ $R_i + R_m \le R_s$;
- $(\mathbf{A_3})$ U is a nearest-neighbor and pairwise potential.

Remark 3.1: $(\mathbf{A_1})$ requires that the mission space be bounded; it is a reasonable assumption and allows one to conclude the convergence to a unique stationary distribution under constant-temperature sampling. $(\mathbf{A_2})$ implies that a node s at x_s sees who would be its neighbors if it moves to $y_s \in F_s(x)$ while other nodes stay put. In $(\mathbf{A_3})$ considering a nearest-neighbor potential enables local evaluation of (6), or local interactions among nodes. Requiring a pairwise potential is critical for the theoretical results of this paper. On the other hand, the class of pairwise potentials can cover a number of interesting problems in swarming, such as rendezvous, dispersion, and formation control.

With $(\mathbf{A_3})$, (6) can be rewritten as

$$P_s^T(x_s, y_s) = \mathbf{1}(y_s \in F_s(x)) \frac{e^{-\frac{U_{\{s\}}(y_s) + \sum_{t \in \Gamma_s(y_s, x_{S\setminus s})} U_{\{s,t\}}(y_s x_t)}{T}}}{\sum_{z_s \in F_s(x)} e^{-\frac{U_{\{s\}}(z_s) + \sum_{t \in \Gamma_s(z_s, x_{S\setminus s})} U_{\{s,t\}}(y_s x_t)}{T}}}, \quad (7)$$

and its local computability is obvious. In (7), $\mathbf{1}(\cdot)$ denotes the indicator function.

The transition kernel $\mathscr{P}_T(x,y) \triangleq Prob(X_{n+1} = y | X_n = x)$ can be obtained from (7):

$$\begin{aligned} \mathscr{P}_T(x,y) &= \prod_{s \in S} P_s^T(x_s, y_s) = \mathbf{1}(y \in F(x)) \cdot \\ &\quad \frac{e^{-\frac{\sum_{s \in S}\left(U_{\{s\}}(y_s) + \sum_{t \in \Gamma_s(y_s, x_{S\setminus s})} U_{\{s,t\}}(y_s x_t)\right)}{T}}}{\sum_{z \in F(x)} e^{-\frac{\sum_{s \in S}\left(U_{\{s\}}(z_s) + \sum_{t \in \Gamma_s(z_s, x_{S\setminus s})} U_{\{s,t\}}(z_s x_t)\right)}{T}}} \quad (8) \\ &= \mathbf{1}(y \in F(x)) \cdot \frac{e^{-\frac{\tilde{H}(x,y)}{T}}}{\sum_{z \in F(x)} e^{-\frac{\tilde{H}(x,z)}{T}}}, \quad (9) \end{aligned}$$

where $\tilde{H}(x,y) \triangleq \sum_{s \in S}\left(U_{\{s\}}(y_s) + \sum_{t \in \Gamma_s(y_s, x_{S\setminus s})} U_{\{s,t\}}(y_s x_t)\right)$. The denominator of (8) is derived from that, for $y \in F(x)$, $\mathscr{P}_T(x,y)$ is proportional to $\tilde{H}(x,y)$, and that $\sum_{z \in F(x)} \mathscr{P}_T(x,z) = 1$.

Define further

$$\begin{aligned} \overline{H}(x,y) &\triangleq \tilde{H}(x,y) + \sum_{s \in S} U_{\{s\}}(x_s) \\ &= \sum_{s \in S}\left(U_{\{s\}}(y_s) + U_{\{s\}}(x_s) + \sum_{t \in \Gamma_s(y_s, x_{S\setminus s})} U_{\{s,t\}}(y_s x_t)\right). \quad (10) \end{aligned}$$

It is easy to see that (9) continues to hold with $\tilde{H}(x,y)$ replaced by $\overline{H}(x,y)$, since all that does is to multiply both the numerator and the denominator by a common factor $e^{-\sum_{s \in S} U_{\{s\}}(x_s)/T}$.

Lemma 3.1: For $y \in F(x)$, the function $\overline{H}$ is symmetric, i.e., $\overline{H}(x,y) = \overline{H}(y,x)$.

Proof. A key observation is that $t \in \Gamma_s(y_s, x_{S\setminus s}) \Rightarrow s \in \Gamma_t(x_t, y_{S\setminus t})$, i.e., node t being a neighbor of node s for the configuration $(y_s, x_{S\setminus s})$ implies that node s is a neighbor of node t for $(x_t, y_{S\setminus t})$. One can then write

$$\begin{aligned} &\overline{H}(x,y) \\ &= \sum_{s \in S}\left(U_{\{s\}}(y_s) + U_{\{s\}}(x_s) + \sum_{t \in \Gamma_s(y_s, x_{S\setminus s})} U_{\{s,t\}}(y_s x_t)\right) \\ &= \sum_{s \in S}\left(U_{\{s\}}(y_s) + U_{\{s\}}(x_s)\right) + \sum_{t \in S} \sum_{s \in \Gamma_t(x_t, y_{S\setminus t})} U_{\{s,t\}}(y_s x_t) \\ &= \sum_{t \in S}\left(U_{\{t\}}(y_t) + U_{\{t\}}(x_t) + \sum_{s \in \Gamma_t(x_t, y_{S\setminus t})} U_{\{t,s\}}(x_t y_s)\right) \\ &= \overline{H}(y,x). \end{aligned}$$

□

B. Stationary Distribution Under Constant-T Sampling

Parallel Gibbs sampling produces a Markov chain $X(n)$ for the swarm configuration. We first characterize the stationary distribution of $X(n)$ for a fixed temperature T. This can then be used to analyze the limiting behavior as $T \to 0$ during simulated annealing.

Theorem 3.1: Let the assumptions $(\mathbf{A_1})-(\mathbf{A_3})$ hold. Under parallel Gibbs sampling with a fixed T, the swarm configuration $X(n)$ has a unique stationary distribution Π_T:

$$\Pi_T(x) = \frac{\sum_{z\in F(x)} e^{-\frac{\overline{H}(x,z)}{T}}}{\sum_{x'}\sum_{z\in F(x')} e^{-\frac{\overline{H}(x',z)}{T}}}. \tag{11}$$

Furthermore, starting from any distribution ν,

$$\lim_{n\to\infty} \nu \mathscr{P}_T^n \to \Pi_T, \tag{12}$$

where $\mathscr{P}_T$ represents the transition matrix determined by (9).

Proof. For a constant T, $X(n)$ generated under Gibbs sampling is a homogeneous Markov chain with transition matrix $\mathscr{P}_T$. From $(\mathbf{A_1})$, there exists a finite integer $\tau > 0$, such that, given any two configurations x and y, the probability of reaching y from x within τ sampling steps is positive. In other words, $\mathscr{P}_T$ has a strictly positive power $\mathscr{P}_T^\tau$. Hence the Markov chain $X(n)$ is ergodic and has a unique, stationary distribution [20]; furthermore, (12) follows.

The only thing remaining to be shown is the explicit form of Π_T. Denote the denominator in (11) as Z_T. For $y \in F(x)$,

$$\begin{aligned}
\Pi_T(x)\mathscr{P}_T(x,y) &= \frac{\sum_{z\in F(x)} e^{-\frac{\overline{H}(x,z)}{T}}}{Z_T} \cdot \frac{e^{-\frac{\overline{H}(x,y)}{T}}}{\sum_{z\in F(x)} e^{-\frac{\overline{H}(x,z)}{T}}} \\
&= \frac{e^{-\frac{\overline{H}(x,y)}{T}}}{Z_T} \qquad (13) \\
&= \frac{\sum_{z\in F(y)} e^{-\frac{\overline{H}(y,z)}{T}}}{Z_T} \cdot \frac{e^{-\frac{\overline{H}(y,x)}{T}}}{\sum_{z\in F(y)} e^{-\frac{\overline{H}(y,z)}{T}}} \\
&= \Pi_T(x)\mathscr{P}_T(x,y), \qquad (14)
\end{aligned}$$

where Lemma 3.1 is used in (13). If $y \notin F(x)$, $\mathscr{P}_T(x,y) = \mathscr{P}_T(y,x) = 0$ and (14) still holds. It is then straightforward to show that Π_T is indeed a stationary distribution:

$$\begin{aligned}
\sum_y \Pi_T(y)\mathscr{P}_T(y,x) &= \sum_y \Pi_T(x)\mathscr{P}_T(x,y) \\
&= \Pi_T(x)\sum_y \mathscr{P}_T(x,y) \\
&= \Pi_T(x),
\end{aligned}$$

since $\sum_y \mathscr{P}_T(x,y) = 1$. □

C. Convergence under Annealing

Let τ be the minimum integer such that all entries of $\mathscr{P}_T^\tau$ are strictly positive. Note that the definition of τ is independent of T. In annealing, the temperature $T(n)$ will drop as a function of time n.

Theorem 3.2: Let the assumptions $(\mathbf{A_1})-(\mathbf{A_3})$ hold. Let $\overline{H}$ be defined as in (10). Define

$$\Delta \stackrel{\triangle}{=} \max_x \max_{y,z\in F(x)} |\overline{H}(x,y) - \overline{H}(x,z)|.$$

Let $T(n)$ be a cooling schedule such that

$$T(n) = T_k, \;\; \tau k \le n < \tau(k+1), \tag{15}$$

where $\{T_k\}$ is a sequence decreasing to 0 and satisfying

$$T(k) \ge \frac{\Delta}{\ln k}. \tag{16}$$

Then for any initial distribution ν on the swarm configuration,

1) $$\lim_{k\to\infty} \nu Q_1 \cdots Q_k \to \Pi_0, \tag{17}$$
   where $Q_i \stackrel{\triangle}{=} \mathscr{P}_{T_i}^\tau$, and Π_0 represents the limit of Π_T, (12), as $T \to 0$;
2) Define $m_0 = \min_x \min_{z\in F(x)} \overline{H}(x,z)$. The support $\mathscr{M}$ of the limiting distribution Π_0 is
   $$\mathscr{M} = \{x : \overline{H}(x,z) = m_0 \text{ for some } z \in F(x)\}. \tag{18}$$

Proof. Claim 1) concerns the characterization of the limiting behavior of $\|\nu Q_1 \cdots Q_k - \Pi_0\|_1$, where $\|\cdot\|_1$ denotes the 1-norm of a vector. The proof uses the contraction property of the Markov kernel Q_k, which is where the annealing schedule (16) comes in. The full proof follows closely the steps in proving Theorem 3.2 in [12], and is omitted here for the interest of brevity.

To establish the support of Π_0, one can rewrite Π_T as

$$\Pi_T(x) = \frac{\sum_{z\in F(x)} e^{-\frac{\overline{H}(x,z)-m_0}{T}}}{\sum_{x'}\sum_{z\in F(x')} e^{-\frac{\overline{H}(x',z)-m_0}{T}}}. \tag{19}$$

As $T \to 0$, $e^{-\frac{\overline{H}(x,z)-m_0}{T}}$ approaches 0 if $\overline{H}(x,z) \neq m_0$, and approaches 1 otherwise. As a result, the numerator of $\Pi_0(x)$, expressed as in (19), will be nonzero if and only if $x \in \mathscr{M}$. Claim 2) follows by noting that the denominator of $\Pi_0(x)$ is always positive and finite. □

Remark 3.2: Theorem 3.2 establishes the convergence behavior of the parallel annealing algorithm for swarm MRFs. The algorithm produces limiting configurations x^* that, with perturbation up to R_m, achieve the minimum of $\overline{H}$, a modified version of the original energy function H. Note the close connection between $\overline{H}$ and H; in particular, $\overline{H}(x,x) = 2H(x)$. In many cases, e.g., the rendezvous problem, the resulting configurations will be precisely characterized by R_m-perturbation of minimal-energy states (in terms of H). While the latter statement may not be rigorous for general cases, the author conjectures that the distance (properly defined) between achieved and desired configurations will still be related to the one-step moving range R_m.

Remark 3.3: Given the speed constraint of a vehicle, R_m is related to the physical time between n and $n+1$, which can be translated to *how frequently* the vehicles observe/communicate with neighbors for making moving

decisions. Theorem 3.2 thus reveals an interesting tradeoff between the optimality and the cost for information gathering.

IV. Simulation Results

Simulation has been further performed to corroborate the analysis and verify the effectiveness of the parallel sampling algorithm. Two examples are presented next: 1) rendezvous, and 2) line formation, both on a 50×50 square lattice. While (16) provides a guidance in choosing the annealing schedule, it is often too conservative. In the simulation, we have adopted schedules of the form: $T(n) = T_0/\ln(n)$, where T_0 is chosen empirically.

A. Rendezvous

In the rendezvous problem, the potential is designed as, for $t \in \Gamma_s(x)$,

$$\begin{aligned} U_{\{s\}}(x_s) &= 0 \\ U_{\{s,t\}}(x_s x_t) &= \begin{cases} 10 & \text{if } \|x_s - x_t\| = 0 \\ -\frac{1}{\|x_s - x_t\|} & \text{otherwise} \end{cases} . \end{aligned}$$

The first equation implies that there is no pre-specified gathering point. By setting the potential of an overlapping pair to be high in the second equation, the algorithm will discourage multiple vehicles from occupying the same cell and thus avoid over-crowding. Fig. 1 shows the snapshots of swarm configurations at different times. The number of nodes was $N_v = 40$. The parameters used in simulation were: $R_s = 13\sqrt{2}+2$, $R_i = 13\sqrt{2}$, $R_m = 2$, and $T_0 = 5$. While the vehicles tended to form two clusters at $n = 200$, they successfully managed to overcome the local minima of potential energy and reached rendezvous at $n = 650$. This example illustrates the advantage of the Gibbs sampling algorithm over the traditional gradient-descent-type algorithm, which would lead to multiple clusters at the steady state.

B. Line Formation

The vehicles are required to form a line that makes a 45° angle with respect to the horizontal axis. The potential is designed as, for $t \in \Gamma_s(x)$,

$$\begin{aligned} U_{\{s\}}(x_s) &= 0 \\ U_{\{s,t\}}(x_s x_t) &= \begin{cases} 0 & \text{if } \|x_s - x_t\| = 0 \\ -\frac{|<x_s - x_t, [1,\ 1]^T>|}{\sqrt{2}\|x_s - x_t\|} & \text{otherwise} \end{cases} , \end{aligned}$$

where $< \cdot >$ indicates the inner product. The potential is essentially a measure of distance between the angle made by the line connecting a pair of neighboring vehicles and 45°. The additive form of potential energy thus encourages nodes to have more neighbors with desired angles and lead to formation of a single line; overlapping nodes, however, are discouraged since a connecting line is not well defined in that case.

Fig. 2 shows that the potential design does lead to the desired formation. Here 50 nodes were simulated, with $R_s = 10\sqrt{2}+3$, $R_i = 10\sqrt{2}$, $R_m = 3$, and $T_0 = 1$. Starting from a random initial configuration, the swarm was self-organized

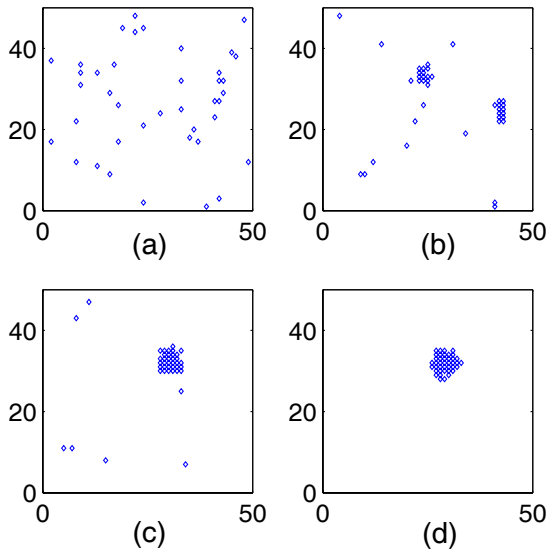

Fig. 1. Snapshots of a swarm of 40 vehicles during rendezvous: (a) Initial configuration; (b) $n = 200$; (c) $n = 300$; (d) $n = 650$.

first into several parallel line segments and finally into a single line. Multiple simulation runs were carried out, starting from different initial configurations. It is interesting to note that, in all cases, the swarm converges to the diagonal line as in Fig. 2. This can be explained by the fact that the diagonal line is the only configuration that can accommodate 50 vehicles with minimum inter-vehicle separation larger than zero, further supporting the global optimization capability of the algorithm. The latter point can be further illustrated with simulation results for 15 vehicles, shown in Fig. 3. Depending on the initial condition, the swarm can evolve into different 45° lines since these configurations would have the same total energy.

Simulation was also performed to study the effect of R_m on final configurations. While the analysis indicates that with larger R_m, the discrepancy between the achieved configuration and the desired one will be larger, it was not clearly observed in simulation, possibly due to the limited number of runs. More extensive simulation is underway for better understanding of this issue.

V. Conclusions

In this paper the parallel Gibbs sampling algorithm for swarming control was analyzed. The explicit expression for the stationary distribution of swarm configuration was derived for the special but popular case of pairwise potential, and the convergence of the algorithm under appropriate annealing schedule was established. It was found that the algorithm minimizes a modified potential energy, where the extent of modification is related to the moving range per sampling step. Simulation results were further presented to demonstrate the effectiveness of the algorithm.

Future work includes extending the analysis to nearest-neighbor potentials of other forms, and to cases involving

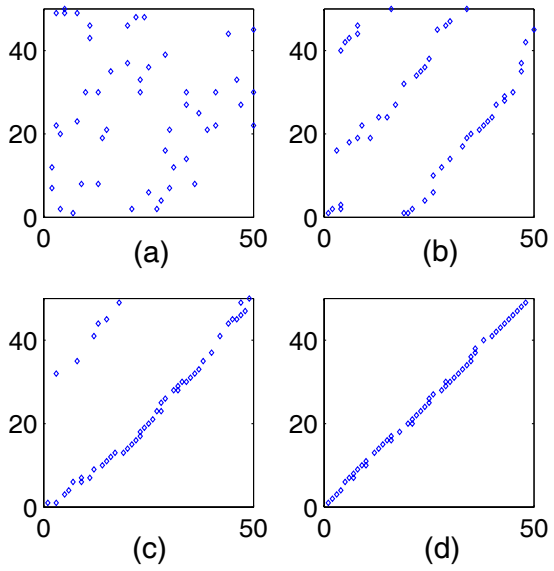

Fig. 2. Snapshots of a swarm of 50 vehicles self-organized into a 45° line: (a) Initial configuration; (b) $n = 10$; (c) $n = 40$; (d) $n = 140$.

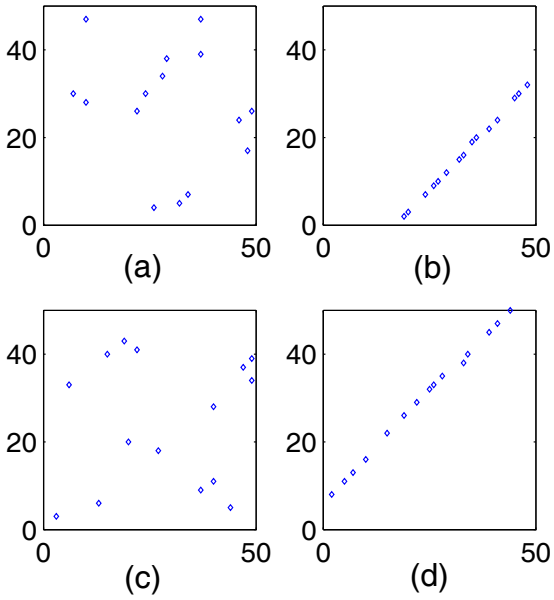

Fig. 3. A swarm of 15 nodes self-organized into different 45° lines: Starting from (a), the swarm evolves into (b); starting from (c), the swarm evolves into (d).

asynchronous sampling. We will also investigate the connection between the parallel Gibbs sampling algorithm, as the time step goes to zero, and the diffusions approach proposed by Tan [21].

REFERENCES

[1] A. Jadbabaie, J. Lin, and A. S. Morse, "Coordination of groups of mobile autonomous agents using nearest neighbor rules," *IEEE Transactions on Automatic Control*, vol. 48, no. 6, pp. 988–1001, 2003.

[2] R. Olfati-Saber and R. M. Murray, "Consensus problems in networks of agents with switching topology and time-delays," *IEEE Transactions on Automatic Control*, vol. 49, no. 9, pp. 1520–1533, 2004.

[3] W. Ren and R. W. Beard, "Consensus seeking in multiagent systems under dynamically changing interaction topologies," *IEEE Transactions on Automatic Control*, vol. 50, no. 5, pp. 655–661, 2005.

[4] L. Moreau, "Stability of multiagent systems with time-dependent communication links," *IEEE Transactions on Automatic Control*, vol. 50, no. 2, pp. 169–182, 2005.

[5] J. Cortes and F. Bullo, "Coordination and geometric optimization via distributed dynamical systems," *SIAM Journal on Control and Optimization*, vol. 44, no. 5, pp. 1543–1574, 2005.

[6] J. S. Baras, X. Tan, and P. Hovareshti, "Decentralized control of autonomous vehicles," in *Proceedings of the 42nd IEEE Conference on Decision and Control*, vol. 2, Maui, Hawaii, 2003, pp. 1532–1537.

[7] P. Ogren, E. Fiorelli, and N. E. Leonard, "Cooperative control of mobile sensor networks: Adaptive gradient climbing in a distributed environment," *IEEE Transactions on Automatic Control*, vol. 49, no. 8, pp. 1292–1302, 2004.

[8] R. Olfati-Saber, "Flocking for multi-agent dynamic systems: Algorithms and theory," *IEEE Transactions on Automatic Control*, vol. 51, no. 3, pp. 401–420, 2006.

[9] J. S. Baras and X. Tan, "Control of autonomous swarms using Gibbs sampling," in *Proceedings of the 43rd IEEE Conference on Decision and Control*, Atlantis, Paradise Island, Bahamas, 2004, pp. 4752–4757.

[10] R. Kindermann and J. L. Snell, *Markov Random Fields and Their Applications*. Providence, RI: American Mathematical Society, 1980.

[11] G. Winkler, *Image Analysis, Random Fields, and Dynamic Monte Carlo Methods : A Mathematical Introduction*. New York: Springer-Verlag, 1995.

[12] W. Xi, X. Tan, and J. S. Baras, "Gibbs sampler-based coordination of autonomous swarms," *Automatica*, vol. 42, no. 7, pp. 1107–1119, 2006.

[13] E. Ising, "Beitrag sur theorie des ferromagnetismus," *Zeit. fur Physik*, vol. 31, pp. 253–258, 1925.

[14] R. Chellappa and A. Jain, *Markov Random Fields: Theory and Applications*. Boston: Academic Press, 1993.

[15] N. Metropolis, A. W. Rosenbluth, M. N. Rosenbluth, A. H. Teller, and E. Teller, "Equations of state calculations by fast computing machines," *Journal of Chemical Physics*, vol. 21, no. 6, pp. 1087–1092, 1953.

[16] S. Geman and D. Geman, "Stochastic relaxation, Gibbs distributions, and the Bayesian restoration of images," *IEEE Transactions on Pattern Analysis and Machine Intelligence*, vol. 6, pp. 721–741, 1984.

[17] S. Kirkpatrick, C. D. Gebatt, and M. Vecchi, "Optimization by simulated annealing," *Science*, vol. 220, no. 4598, pp. 671–680, 1983.

[18] J. Cortes, S. Martinez, and F. Bullo, "Robust rendezvous for mobile autonomous agents via proximity graphs in arbitrary dimensions," *IEEE Transactions on Automatic Control*, vol. 51, no. 8, pp. 1289–1298, 2006.

[19] M. Mesbahi, "On state-dependent dynamic graphs and their controllability properties," *IEEE Transactions on Automatic Control*, vol. 50, no. 3, pp. 387–392, 2005.

[20] R. Horn and C. R. Johnson, *Matrix Analysis*. New York: Cambridge University Press, 1985.

[21] X. Tan, "Self-organization of autonomous swarms via Langevin equation," in *Proceedings of 46th IEEE Conference on Decision and Control*, New Orleans, LA, 2007, to appear.